

**Supplementary Information:**

**A ruthenium polypyridyl intercalator stalls DNA replication forks, radiosensitizes human cancer cells and is enhanced by Chk1 inhibition**

Martin R. Gill<sup>1</sup>, Siti Norain Harun<sup>2</sup>, Swagata Halder<sup>1</sup>, Ramon A. Boghoozian<sup>1</sup>, Kristijan Ramadan<sup>1</sup>, Haslina Ahmad<sup>2</sup> and Katherine A. Vallis<sup>1</sup>\*

1 CRUK/MRC Oxford Institute for Radiation Oncology, Department of Oncology, University of Oxford, Oxford, UK

2 Department of Chemistry, Faculty of Science, Universiti Putra Malaysia, Malaysia

\* email: katherine.vallis@oncology.ox.ac.uk

**Contents:**

**Supplementary Figures 1 – 14 (p2)**

**Supplementary Tables 1 and 2 (p13)**

**Supplementary Methods (p14)**

**Supplementary References (p15)**

Supplementary Figures:

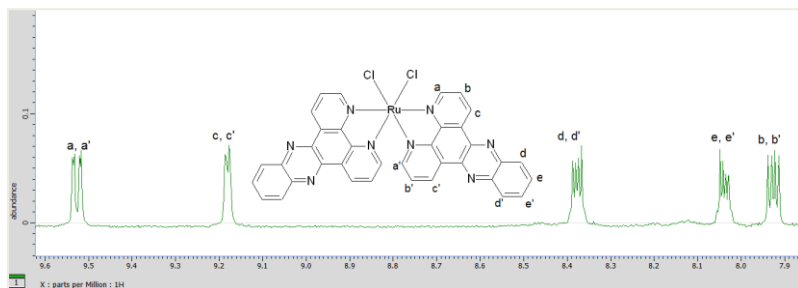


Figure S1. <sup>1</sup>H NMR spectrum of Ru(dppz)<sub>2</sub>Cl<sub>2</sub> in C<sub>2</sub>D<sub>6</sub>OS.

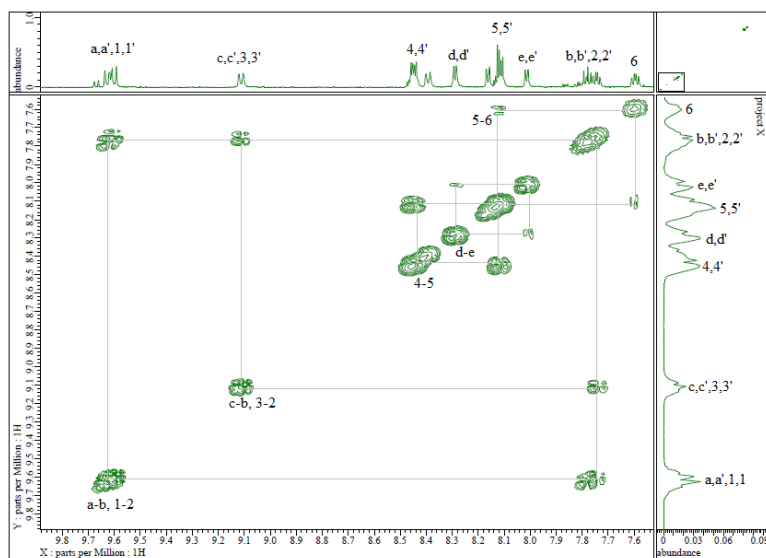
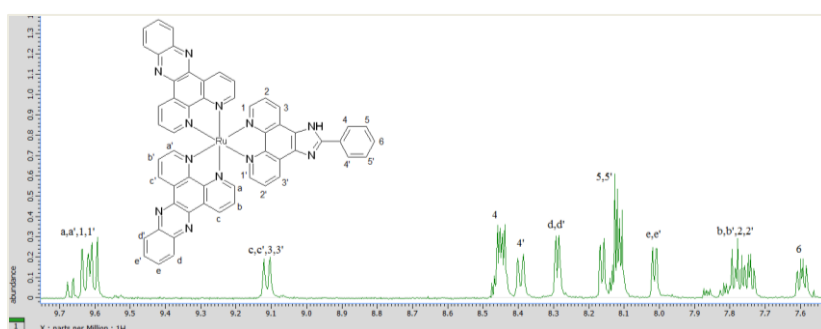
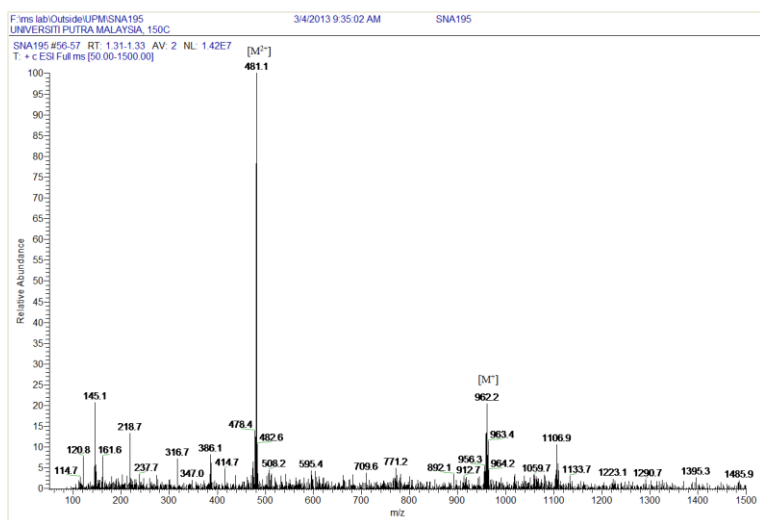
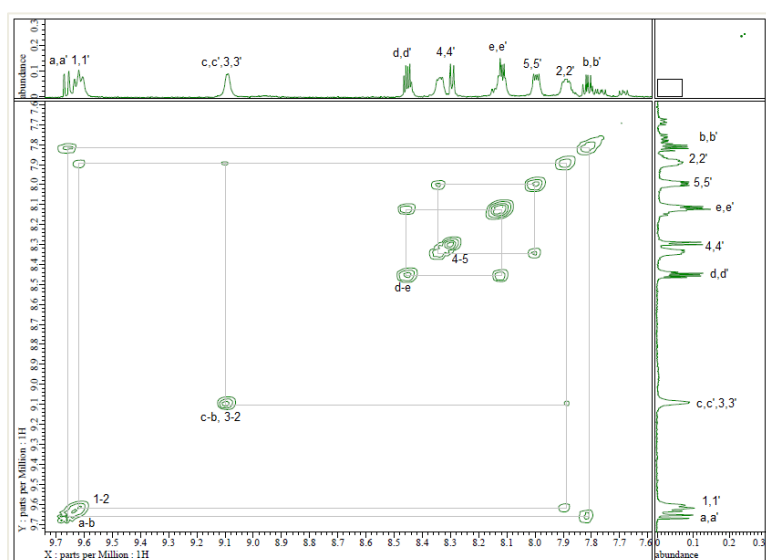
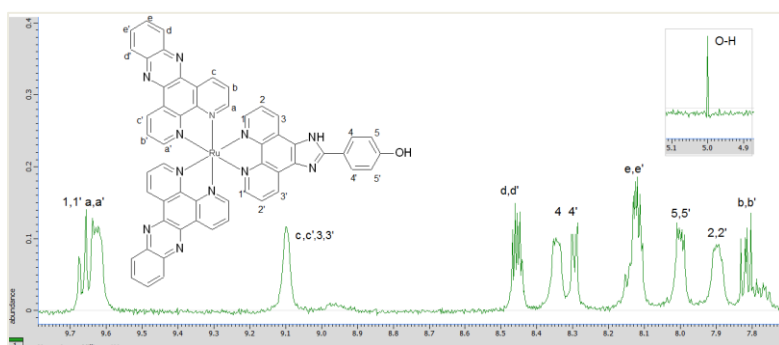


Figure S2. <sup>1</sup>H NMR (top) and 2D COSY <sup>1</sup>H NMR (bottom) of [Ru(dppz)<sub>2</sub>PIP]<sup>2+</sup> (complex 1) in CD<sub>3</sub>CN.



**Figure S3.** ESI mass spectrum of **1**.



**Figure S4.**  $^1\text{H}$  NMR of  $[\text{Ru}(\text{dppz})_2\text{HPIP}]^{2+}$  (complex **2**) (top) and 2D COSY  $^1\text{H}$  NMR (bottom) in  $\text{CD}_3\text{CN}$ .

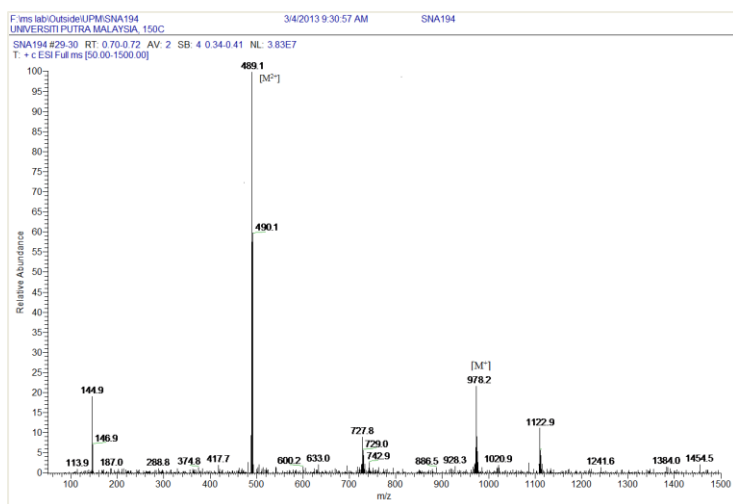


**Figure S5.** ESI mass spectrum of **2**.

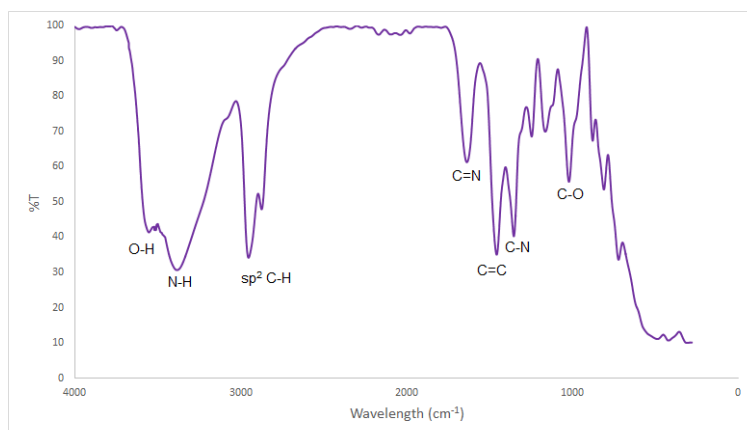


**Figure S6.** FT-IR spectrum of **2**.

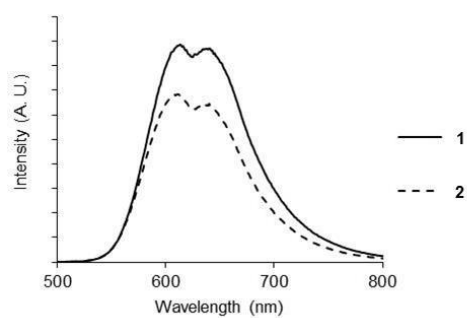


**Figure S7.** Luminescence emission spectra of 10  $\mu$ M **1** and **2** in acetonitrile at room temperature (excitation wavelength = 460 nm).

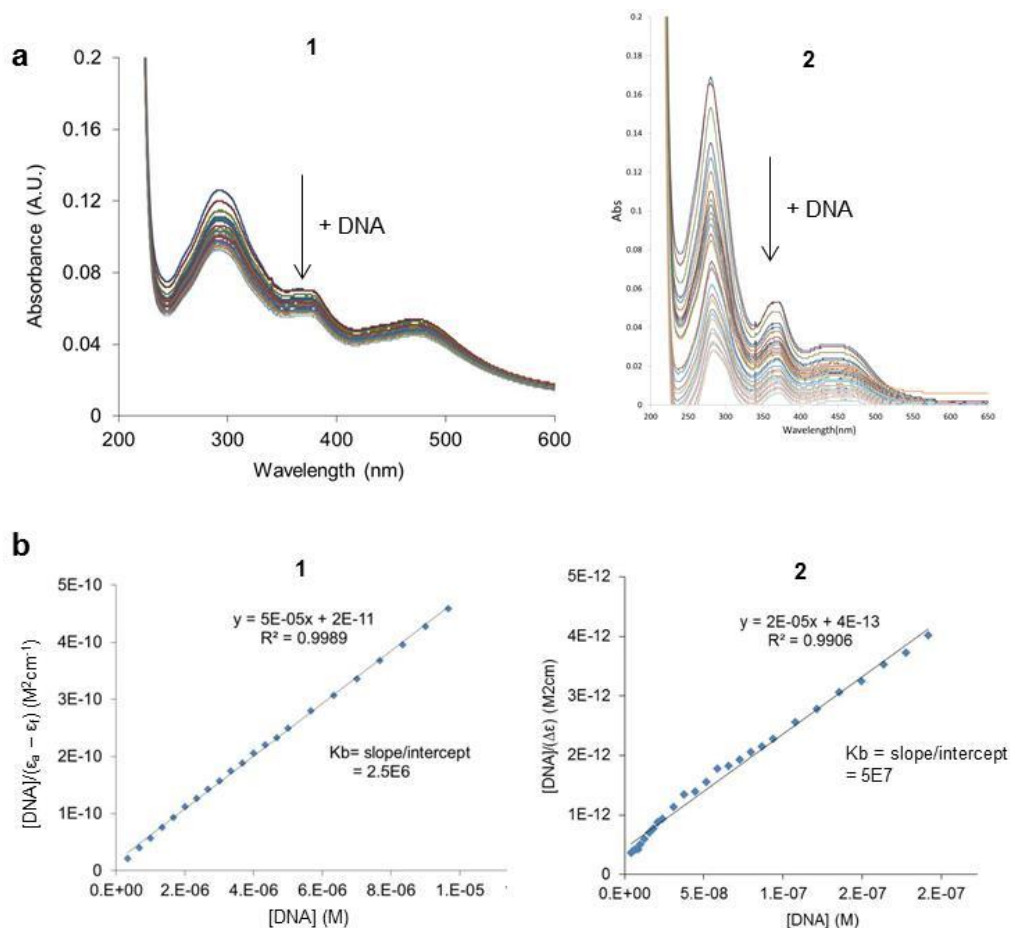


**Figure S8.** (a) Changes in UV-visible absorption spectrum of **1** or **2** with addition of DNA, indicating hypochromicity with increasing DNA concentration (buffer: 5 mM Tris-HCl, 25 mM NaCl, pH 7.2, 0.5 % DMSO). (b) Example fits of  $[DNA]/(\epsilon_a - \epsilon_f)$  versus  $[DNA]$  for hypochromic shifts of **1** and **2** with DNA.  $K_b$  is provided by the slope to intercept ratio.  $[DNA]$  = concentration of DNA in base pairs,  $\epsilon_a$  and  $\epsilon_f$  are apparent extinction coefficient for free complex and  $A_{\text{obs}}/[M]$  respectively.

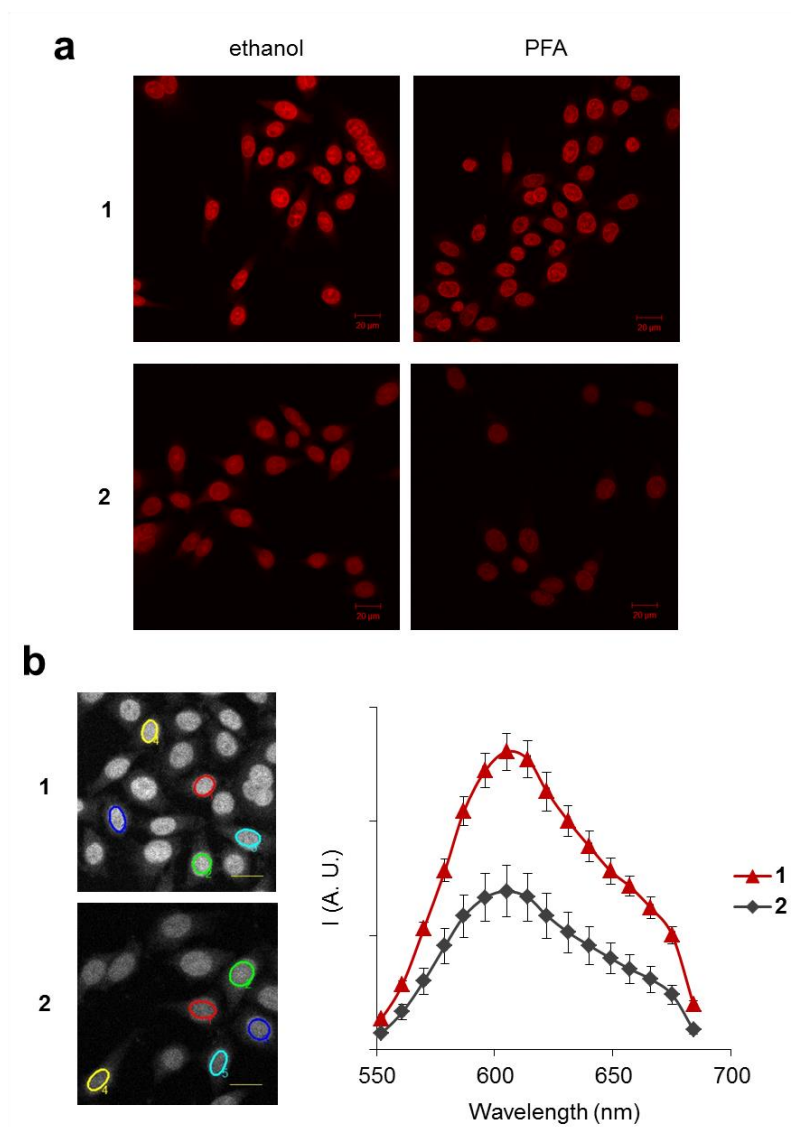


**Figure S9.** (a) Confocal micrographs of HeLa cells fixed with ethanol (70 %) or PFA (4% + 0.1 % Triton for membrane permeabilisation) showing cell nuclei stained by **1** or **2** (100  $\mu$ M, 10 mins). (b) Emission profiles of **1** and **2**-stained HeLa cell nuclei. Data average of five nuclei stained (indicated by \*, left hand images). Excitation wavelength = 488 nm. Identical microscope settings used for image acquisition.

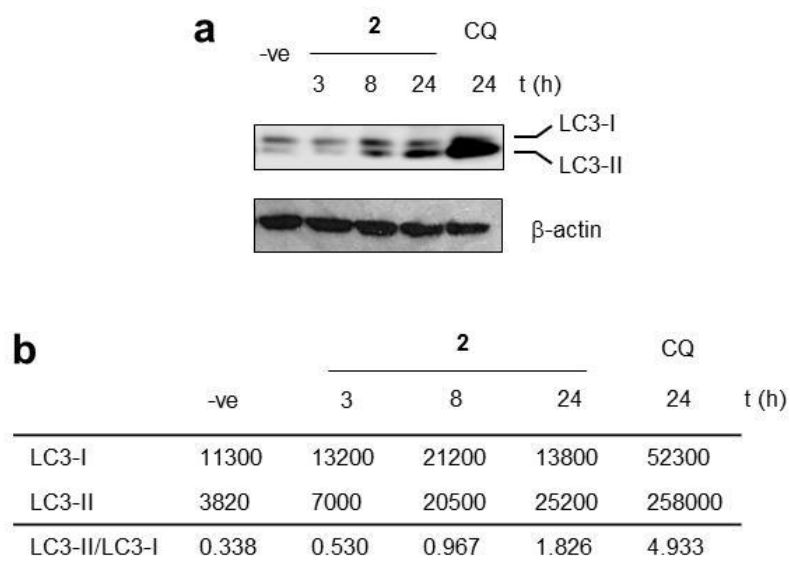


**Figure S10.** (a) Immunoblotting analysis of lysates derived from HeLa cells treated with **2** (20  $\mu$ M) for 3-24 h for increased levels of autophagy marker LC3-II (top blot, bottom band).  $\beta$ -actin levels were probed as a loading control. HeLa cells treated in parallel with chloroquine (CQ, 10  $\mu$ M, 24 h) were employed as a positive control for LC3-II generation (see Supplementary Reference 1). (b) Densitometry of Western blots from (a). The increase in LC3-II/LC3-I ratio provides evidence of autophagy (see CQ data and supplementary reference 2).

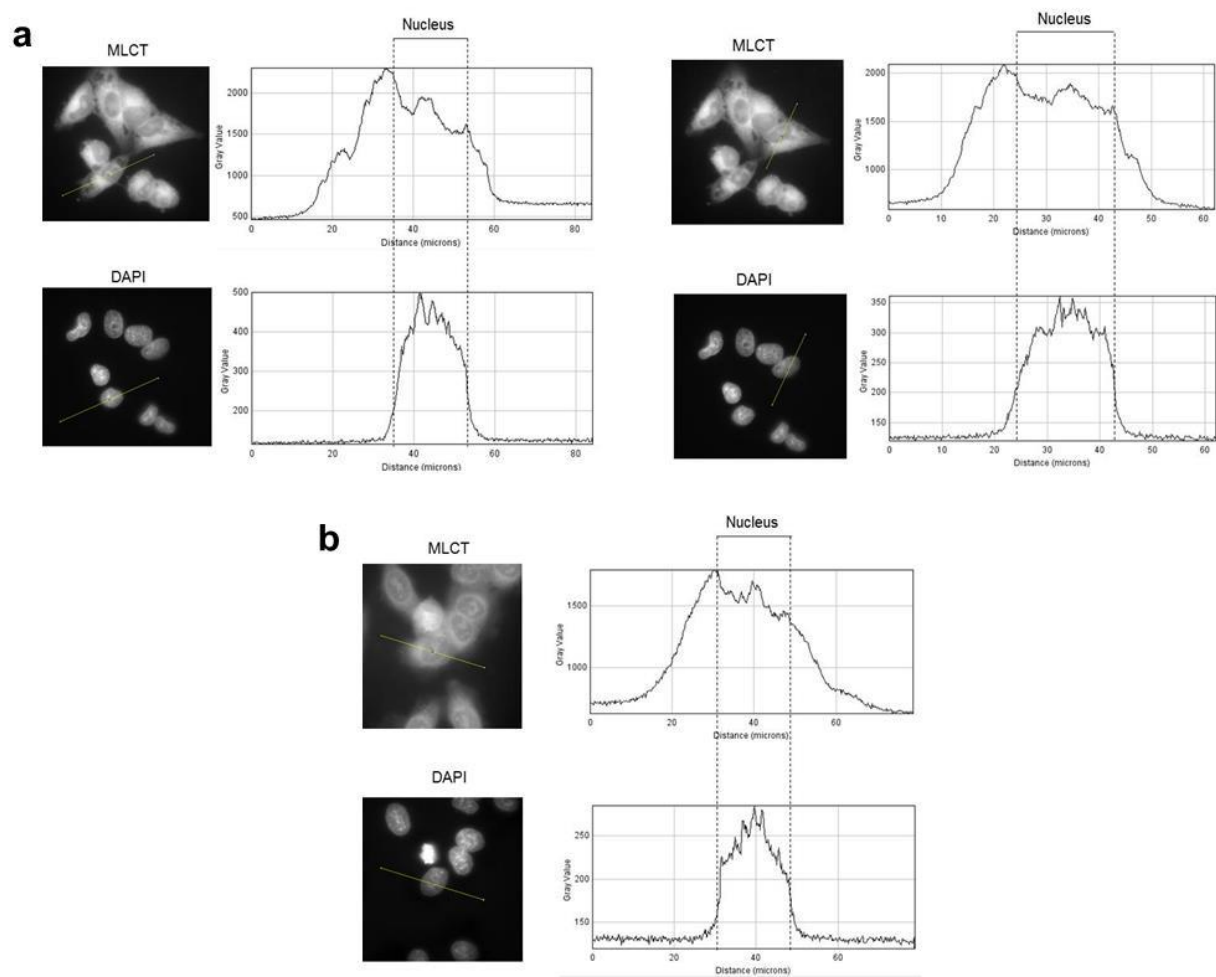


**Figure S11.** MLCT emission profiles of HeLa cells treated with **1** (a) or **2** (b) (40  $\mu$ M, 24 h). DAPI emission profiles are included for comparison.



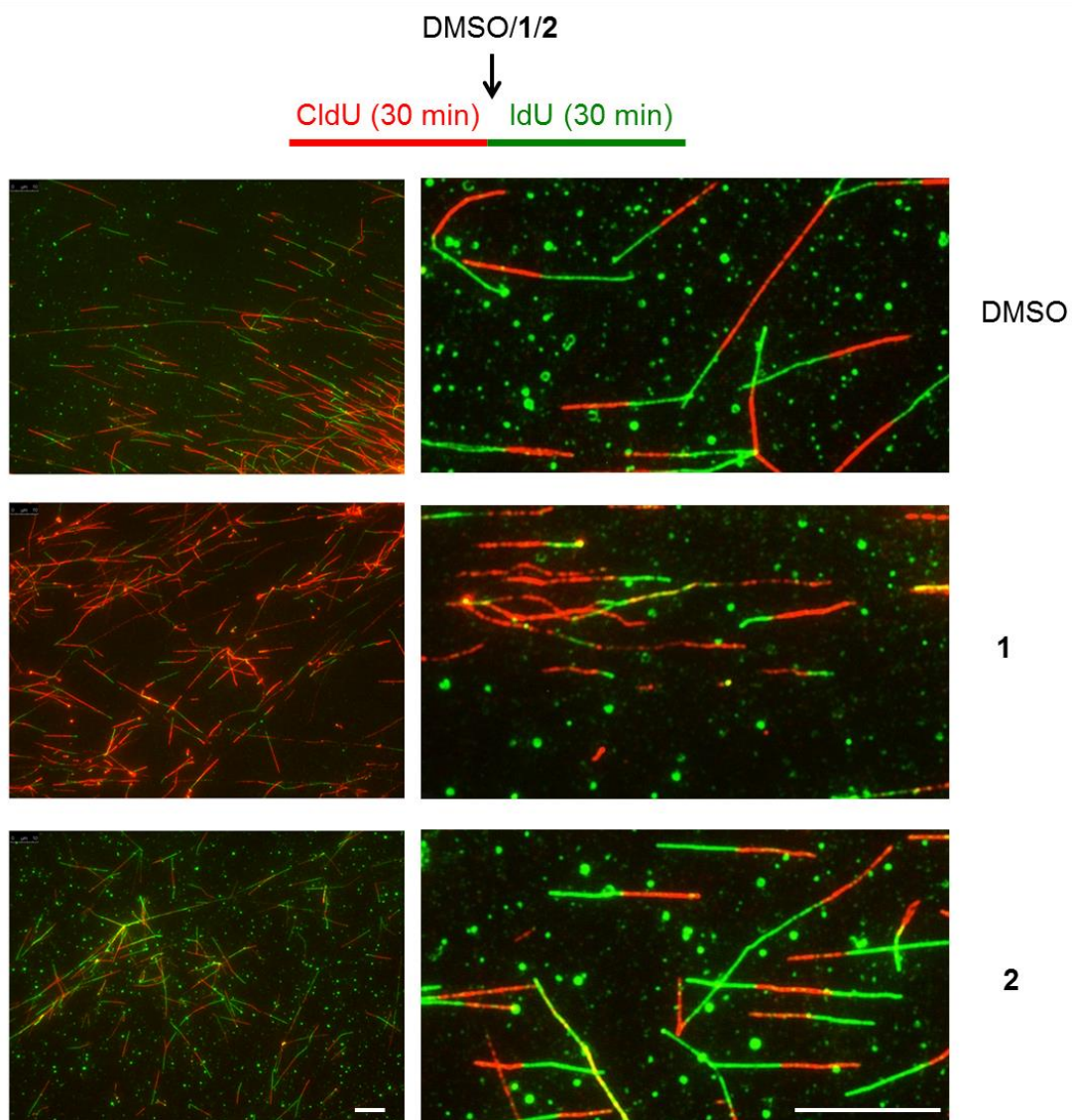


**Figure S12.** Representative DNA fibres labelled sequentially with CldU (red) and IdU (green) when the incorporation of the second synthetic nucleotide IdU (green) was in the absence or presence of **1** or **2** (40  $\mu$ M). Scale bars = 10  $\mu$ m. Note that IdU tracts (green) are shorter - or absent - with the addition of **1** compared to either DMSO (mock) or **2** treatment, indicating replication fork slowdown and stalling by complex **1**.

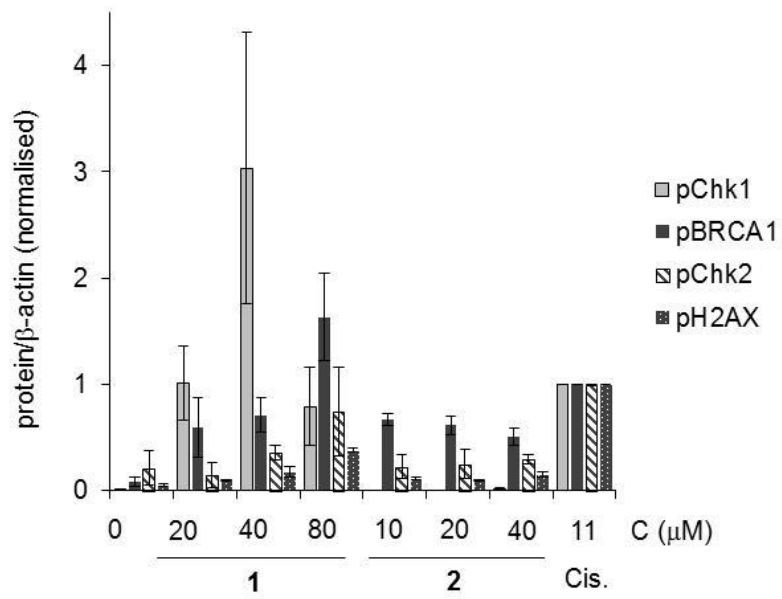


**Figure S13.** Densitometry of Western Blots of HeLa cell lysates treated with **1**, **2** or cisplatin (24 h). Phospho-DDR protein levels (pChk1, pBRCA1, pChk2, pH2AX) divided by protein loading controls ( $\beta$ -actin) and normalised to cisplatin results. Data average of two technical repeats  $\pm$  SD.

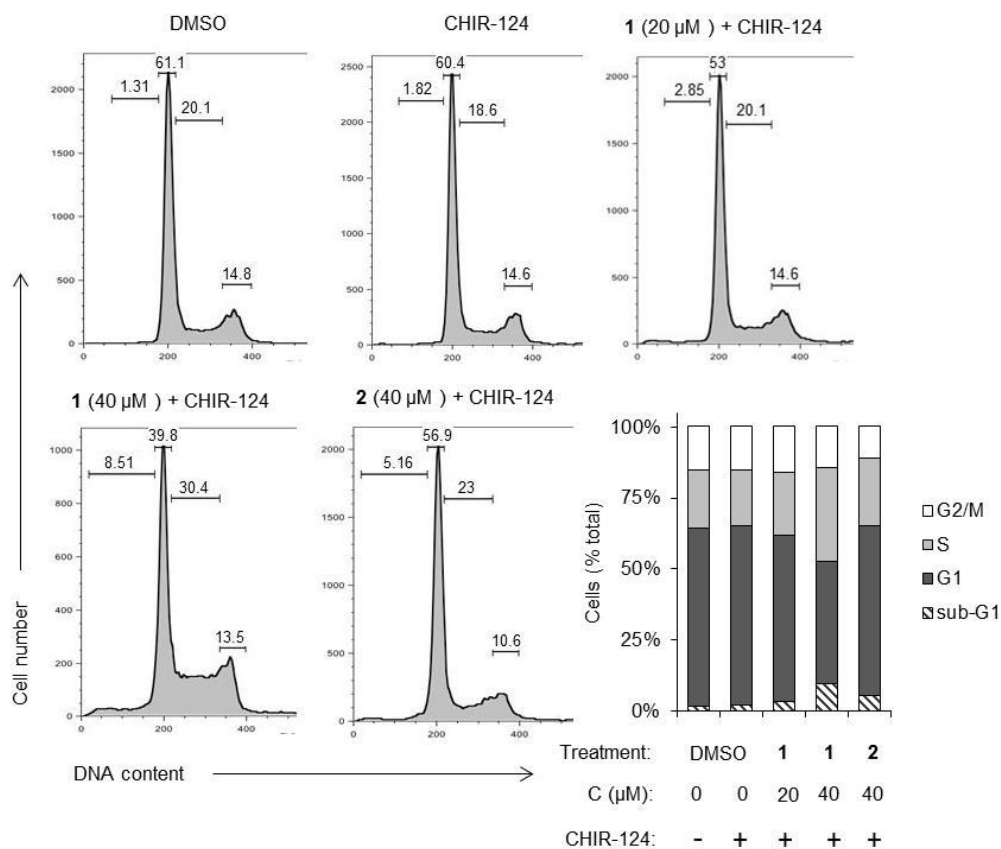


**Figure S14.** Cell-cycle distribution for HeLa cells incubated with **1** or **2** + CHIR-124 (500 nM) for 24 h. DNA content was quantified using propidium iodide (PI) and analysed by flow cytometry. Data summarised in bottom-right.

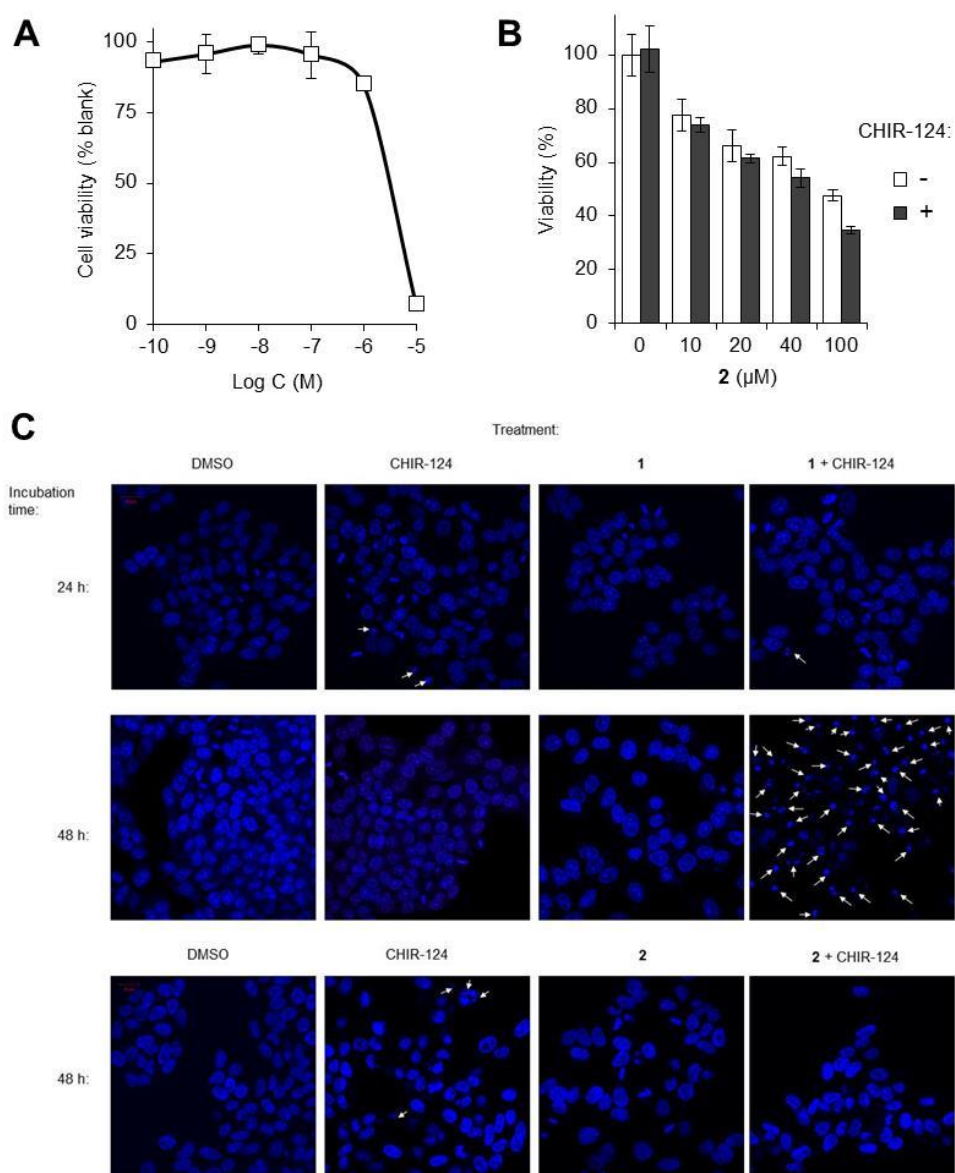


**Figure S15.** (a) Impact of Chk1 inhibitor CHIR-124 on cell viability of HeLa cells. Resultant cell viabilities assessed by MTT assay (in triplicate, +/- S.D.) after 48 h exposure. (b) HeLa cell viability after incubation with **2** in the absence or presence of Chk1 inhibitor CHIR-124 (500 nM) for 48 h constant exposure. (c) HeLa cells treated with either 40 µM **1** or **2** in the absence or presence of CHIR-124 (500 nM) for 24 h or 48 h. Late apoptotic nuclear morphology (pyknosis and/or karyorrhexis) indicated by arrows. Micrographs are representative of two independent experiments.

## Supplementary Tables:

**Table S1.** UV-Vis absorbance data for **1** and **2**.\*

Complex	$\lambda_{\max}$ (nm)	$\epsilon$ ( $M^{-1}cm^{-1}$ )	Assignment
<b>1</b>	458	5100	MLCT
	358	8470	$\pi \rightarrow \pi^*$
	280	37100	$\pi \rightarrow \pi^*$
<b>2</b>	458	10600	MLCT
	358	24580	$\pi \rightarrow \pi^*$
	280	86600	$\pi \rightarrow \pi^*$

\*In acetonitrile at 293 K. MLCT = metal to ligand charge-transfer.

**Table S2.** Radiosensitization data for **1** and **2** in HeLa cells.

	LD <sub>10</sub> (Gy)	DEF	Radiosensitivity (AUC)	RER
DMSO	6.7	-	3.83	-
<b>1</b>	4.5	1.49	2.59	1.48
<b>2</b>	5.9	1.14	3.39	1.13

Survival variables LD<sub>10</sub> (10 % lethal dose) and radiosensitivity, which is expressed as the area under the survival curve (AUC), derived from linear regression analyses of survival curves ( $R^2$  values  $\geq$  0.989 for all fits). Dose enhancement factor (DEF) = LD<sub>10</sub> [without complex]/LD<sub>10</sub> [with complex]. Radiation enhancement ratio (RER) = radiosensitivity [without complex]/radiosensitivity [with complex].

## Supplementary Methods

### Instrumentation

NMR spectra for  $^1\text{H}$  and 2D-COSY were recorded on a JEOL ECX500 FT NMR spectrometer.

Deuterated  $\text{CDCl}_3$ , DMSO or  $\text{CD}_3\text{CN}$  were used as solvents. Chemical shifts are relative to tetramethylsilane (TMS) as reference and are reported in ppm with coupling constants in Hertz (Hz).

The multiplicities of peaks in  $^1\text{H}$  NMR spectra were reported using abbreviation as follows: s - singlet, d - doublet, t - triplet, m - multiplet. Electrospray ionization mass spectra (ESI-MS) were measured on a Finnigan TSQ7000 mass spectrometer. Elemental analysis (C, H, N and O) were carried out using Leco CHNS-932 Elemental Analyzer. UV-Visible (UV-Vis) spectra were recorded on a Shimadzu H.U.V.1650 PC UV-Visible spectrophotometer for the wavelength range of 200-600 nm. Emission spectra were recorded over the range of 500-850 nm with excitation wavelength of 460 nm on a Shimadzu RF-5301 PC Spectrofluorophotometer.

### Octanol/water partition coefficients

Octanol/water partition coefficients (Log P values) were calculated the “shake flask” method, where the concentration in each phase was determined by UV-Vis spectroscopy.  $\text{Log P} = \log \left( \frac{[\text{octanol}]}{[\text{water}]} \right)$ . The calculated log P value for mitoxantrone was determined using Molinspiration Chemoinformatics software ([www.molinspiration.com](http://www.molinspiration.com)).

### Fixed tissue and fixed cell imaging

Sample preparation:

i) Frozen sections: MDA-MB-468 cell-line derived tumour xenografts and normal liver samples were a generous gift from Dr L. Song. Sections were fixed in 4 % paraformaldehyde (PFA) for 10 minutes, followed by permeabilisation in 1 % Triton/PBS for 10 minutes. Slides were incubated with **1** (0.1 – 5 mM, 1 h). Next, Sections were washed in PBS for 2 x 3 minutes and subsequently mounted with Vectashield® mounting medium (Vector Laboratories, Burlingame, CA) and coverslips. ii) Formalin-fixed paraffin-embedded sections: SQ20B cell-line pellets were deparaffinised using xylene (Sigma)

at room temperature for 2 x 3 minutes. Graded ethanol (Sigma) series comprising of 100 %, 95 %, 70 % and 50 % was used to rehydrate tumour sections, followed by permeabilisation in 1 % Triton/PBS for 10 minutes. Slides were incubated with **1** (5 mM, 1 h), washed with PBS (2 x 3 mins) and sections were mounted with mounting medium (Vector Laboratories) and coverslips. iii) Monolayer cultures: HeLa or MDA-MB-468 cells were fixed with paraformaldehyde (4 %, 10 mins) and additionally permabilised with Triton (0.1 %, 10 mins) before staining with **1** or **2** (100 µM, 1 h). Samples were washed with PBS and, where stated, co-stained with DAPI (500 nM, 2 min).

#### Microscopy:

Samples were visualised on Zeiss LSM 780 META inverted confocal microscope and x40 or x63 oil-immersion objectives, where **1** and **2** were excited with an Ar-ion laser at 488 nm and emission collected at 600-650 nm. Lambda stacking experiments employed collecting emission intensity data from 552-684 nm at intervals of 9 nm. DAPI was detected as standard.

#### Supplementary References

1. Ni, H.-M. *et al.* Dissecting the dynamic turnover of GFP-LC3 in the autolysosome. *Autophagy* **7**, 188-204 (2011)
2. Kabeya, Y. *et al.* LC3, GABARAP and GATE16 localize to autophagosomal membrane depending on form-II formation. *J. Cell Sci.* **117**, 2805-2812 (2004)